Reconstruction of Cole-Cole Parameters from IP Induction Sounding Data

I.N. Yeltsov, M.I. Epov and E.Yu. Antonov

Electromagnetic Fields Laboratory, Institute of Geophysics, Siberian Branch Russian Academy of Science,
630090 pr. Akademika Koptyuga, 3, Novosibirsk, Russia.

Abstract: *This paper deals with the non-stationary electromagnetic response to the inductive excitation of a medium containing a layer with the frequency-dependent dispersion of the electrical resistivity. The problem of reconstruction of the inductive induced polarization parameters is solved in the context of the well-known Cole-Cole model. The algorithm of solving inverse problem is based on the Nelder and Mead modified method. The algorithm tested for synthetic models, which are typical for the ore body prospecting, has shown the high effectiveness of the non-linear methods to recover the complex multi-parameter models. The error in the estimation of the induced polarization parameters is less than 3 per cent as it is shown by some examples.*

INTRODUCTION

The study of polarizable geological objects is a new research direction in the high-resolution electromagnetic exploration. This new method is employed when studying the induced polarization (IP) parameters of rocks along with traditionally used resistivity. The polarization parameters are closely connected with material properties of a geological medium; therefore, the reliability of determination of medium properties is increased when these parameters are used (Flis *et al.*, 1989, Smit and West, 1989).

The main impediment to introduction of the new method is in the absence of technology for solving an inverse problem of high-resolution electromagnetic exploration. An attempt to develop such a technology based on the optimization approach within the framework of statistical interpretation theory has been made in the paper. The feature of the present research is in using induction sources and receivers of a signal, while the most of previous works devoted to the study of IP effects dealt with galvanic systems of measurements.

STATEMENT OF THE PROBLEM

Let us begin with the theoretical base of the method for solving the direct problem in a horizontally layered medium, taking into account the frequency dependence of layer resistivity. Maxwell equations in quasi-stationary approach are

$$\text{rot } \mathbf{H} = \sigma(t)\,\mathbf{E} + \mathbf{J}(x,y,z,t) \qquad (1)$$

$$\text{rot } \mathbf{E} = -\mu_0 \frac{\partial \mathbf{H}}{\partial t}, \qquad (2)$$

$$\text{div } \mathbf{E} = 0, \quad \text{div } \mathbf{H} = 0. \qquad (3)$$

In these equations $\mathbf{j}(x,y,z,t)=\mathbf{J}(x,y,z).u(t)$ is the external current density, σ is electrical conductivity, μ is magnetic permeability. When the time dependence is given as $e^{-i\omega t}$, the Fourier transformation are defined as:

$$\vec{F}^*(\omega) = \int_\infty^\infty \vec{F}(t)e^{i\omega t}dt$$

Maxwell equations in the frequency domain are:

$$\text{rot } \mathbf{H}^* = \sigma^*(\omega)\,\mathbf{E}^* + \mathbf{j}(x,y,z,) \qquad (4)$$

$$\text{rot } \mathbf{E}^* = i\omega\mu_0\,\mathbf{H}^* \qquad (5)$$

In particular, the voltage of the infinity current is described as a step-function

$$u(t)=\begin{cases} 1, t \le 0 \\ 0, t > 0 \end{cases}$$

and its spectrum is

$$u^*(\omega) = -1/i\omega$$

Thus, the response in the frequency domain can be transformed in the time domain by using the following expression:

$$F(t) = \frac{1}{2\pi} \int_{-\infty}^{\infty} F^*(\omega)\, u^*(\omega)\, e^{-i\omega t}\, d\grave{u} \qquad (6)$$

Therefore, we have to solve a problem in the frequency domain. Let us write z - components of the equations (1) and (2) in the layer of number *j*, which does not contain any sources:

$$\begin{cases} \dfrac{\partial H_y}{\partial x} - \dfrac{\partial H_x}{\partial y} = \sigma_j E_z, \\[2mm] \dfrac{\partial E_y}{\partial x} - \dfrac{\partial E_x}{\partial y} = i\omega\mu_0 H_z, \\[2mm] \dfrac{\partial H_x}{\partial x} + \dfrac{\partial H_y}{\partial y} = -\dfrac{\partial H_z}{\partial z}, \\[2mm] \dfrac{\partial E_x}{\partial x} + \dfrac{\partial E_y}{\partial y} = -\dfrac{\partial E_z}{\partial z}. \end{cases} \qquad (7)$$

Two-dimensional forward and inverse Fourier-transforms of function *f(x,y,z)* through the coordinates *x*, y are determined by the expressions:

$$f^*(\xi,\eta,z) = \int_{-\infty}^{\infty}\int_{-\infty}^{\infty} f(x,y,z)\, e^{-i\xi x}\, e^{-i\eta y}\, dx\, dy, \qquad (8)$$

$$f(x,y,z) = \frac{1}{(2\pi)^2} \int_{-\infty}^{\infty}\int_{-\infty}^{\infty} f(\xi,\eta,z)\, e^{i\xi x}\, e^{i\eta y}\, d\hat{\imath}\, d\c{c}. \qquad (9)$$

Fourier images of all horizontal components of fields can be obtained from the Fourier images of vertical components E_z^+, H_z^+ by the inverse Fourier transformation (9) of the system (7):

$$H_x^* = \frac{i\eta}{\xi^2+\eta^2}\sigma_k E_z^* + \frac{i\xi}{\xi^2+\eta^2}\frac{\partial H_z^*}{\partial z},$$

$$H_y^* = -\frac{i\xi}{\xi^2+\eta^2}\sigma_k E_z^* + \frac{i\eta}{\xi^2+\eta^2}\frac{\partial H_z^*}{\partial z}, \qquad (10)$$

$$E_x^* = \frac{i\xi}{\xi^2+\eta^2}\frac{\partial E_z^*}{\partial z} + \frac{i\eta}{\xi^2+\eta^2}i\omega\mu_k H_z^*,$$

$$E_y^* = \frac{i\eta}{\xi^2+\eta^2}\frac{\partial E_z^*}{\partial z} - \frac{i\xi}{\xi^2+\eta^2}i\omega\mu_k H_z^*.$$

In Equations (10) $\lambda^2 = \xi^2 + \eta^2$ is the square of spatial frequency. Thus, to obtain the field of any source, it is sufficient to derive the spatial Fourier images of their vertical components (Epov and Yeltsov, 1991).

Taking into account a continuity of horizontal components E_x^+, E_y^+ and expression (7), we obtain the final system of boundary conditions:

$$\left[\sigma E_z^+\right]\Big|_{z=z_j} = 0, \quad \left[\frac{\partial E_z^+}{\partial z}\right]\Big|_{z=z_j} = 0, \quad (j=1,...,n). \qquad (11)$$

$$\left[\mu H_z^+\right]\Big|_{z=z_j} = 0, \quad \left[\frac{\partial H_z^+}{\partial z}\right]\Big|_{z=z_j} = 0, \quad (j=1,...,n). \qquad (12)$$

Components E_z^+ and H_z^+ (below denoted as *F*) in each layer of a medium, which does not contain any sources, satisfy the homogeneous Helmholtz equation:

$$\nabla^2 F + p_j^2 F = 0. \qquad (13)$$

where
$p_j^2 = \lambda^2 + k_j^2,\ k_j^2 = -i\omega_j\mu_j\sigma_j(\omega),\ \mathrm{Re}(k_j) > 0,\ j=1,.....,n+1$

The electrical conductivity $\sigma_j(\omega)$ is considered as a complex function depending on frequency. The functions E_z^+ and H_z^+ satisfy conditions of radiation at infinity as well.

If the layer *m* contains an external source, the solution is represented by the sum of fields from the source in a homogeneous medium with parameters of the corresponding layer $\mathbf{E}^0$, $\mathbf{H}^0$ and anomalous fields $\mathbf{E}^0$, $\mathbf{H}^0$:

$$\mathbf{E} = \mathbf{E}^0 + \mathbf{E}^a,\ \mathbf{H} = \mathbf{H}^0 + \mathbf{H}^a \qquad (14)$$

In this case, the boundary conditions (11) and (12) on *m*- and (*m + 1*)-interfaces become non-uniform.

To construct array of loop-loop configuration and to calculate the responds for layered medium, we have used the integral:

$$\frac{\partial B_z}{\partial t} = \frac{1}{2\pi} \int_{-\infty}^{\infty} \frac{e^{-i\omega t}}{-i\omega} \iint_{L_1 L_2} A_{L_1 L_2}^H(\omega)\, dl_1 dl_2 d\omega$$

where $A_{L_1 L_2}^H$ is the magnetic mode of electrical dipoles constructing loop-loop array, L_1, L_2 are the contour of transmitter and receiver loops.

Thus, the physical phenomenon of the "induced polarization" is treated where as the low-frequency dispersion of electrical resistivity of earth layers, that is the dependence of resistivity on frequency. Such an approach is sufficient for the present research, as that is confirmed by numerous full-scale surveying data. Therefore, we can take an advantage of the known empirical frequency dependencies. In this work, we apply the well-known Cole-Cole model (Svetov *et al.*, 1995):

$$\begin{cases} \rho(-i\omega) = \dfrac{\rho_0 + \rho_\infty(-i\omega\tau_\rho)^c}{1+(-i\omega\tau)^c} = \rho_0\left[1 - m\dfrac{(-i\omega\tau_\rho)^c}{1+(-i\omega\tau_\rho)^c}\right], \\[4mm] \sigma(-i\omega) = \dfrac{\sigma_0 + \sigma_\infty(-i\omega\tau_\sigma)^c}{1+(-i\omega\tau_\sigma)^c} = \sigma_0\left[1 - \dfrac{m}{1+(-i\omega\tau_\sigma)^c}\right]. \end{cases}$$
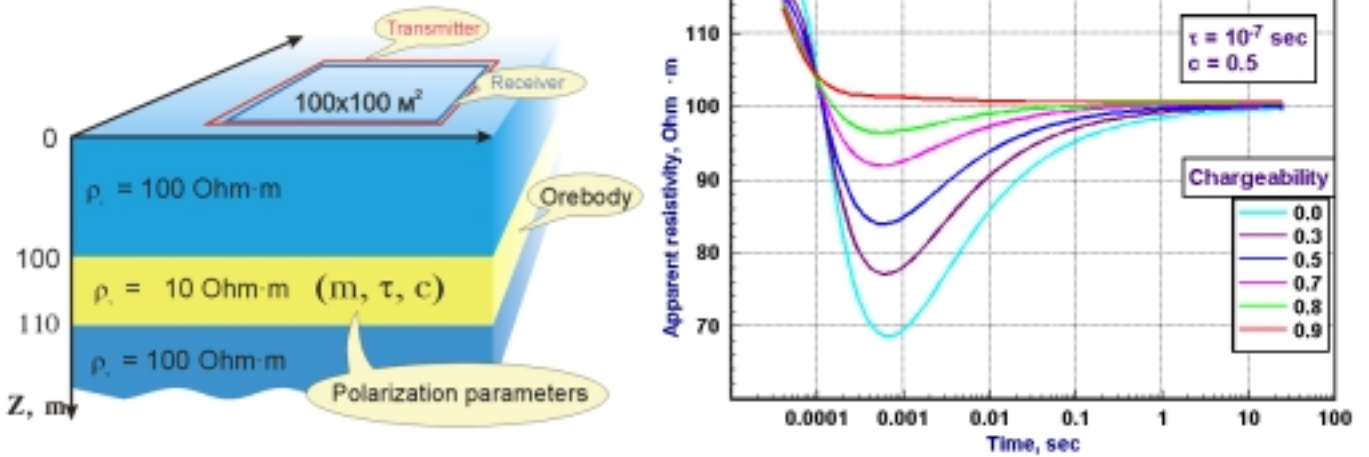
FIG. 1. Geoelectrical model (on the left) and apparent resistivity data over an ore body with various values of parameter m (on the right).
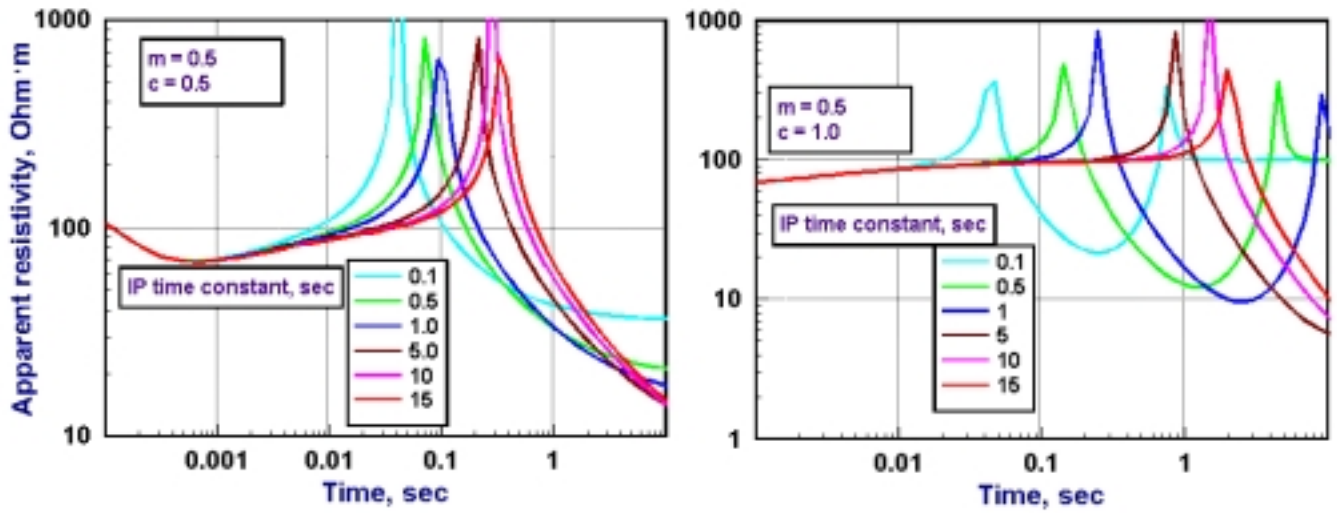

FIG. 2. Apparent resistivity data over an ore body with various values of relaxation time $c = 0.5$ (on the left) and $c = 1.0$ (on the right).

where m is the chargeability parameter, which varies in the range of $(0,1)$, c is the frequency dependence, the values $c = 0.5$ and c = 1 are usually used; τ τ is the time constant, and $\tau_{\rho} = \tau_{\sigma}/(1 - m)^{1/c}$.

ANALYSIS OF THE RESULTS

We consider the geoelectrical model of an ore body (Fig. 1). The ore body is located at the depth $Z_1 = 100$ m, its resistivity (ρ_2) is equal to 10 ohm·m and thickness is 10 m. The object is characterised by Cole-Cole parameters m, c, τ. The excited current of transmitter in the time domain is represented by a step-function. The excitation and measurement of electromagnetic field are carried out by a loop-loop array (loop side size is 100 m). The following expression is used as the apparent resistivity definition:

$$\rho_{\tau} = [\mu^{5/3} (0.4)^{2/3} /(4\pi t^{5/3})][M /(\partial B_z / \partial t)]^{2/3}$$

where M is the moment.

We consider behaviour of an apparent resistivity $\rho\tau$ with respect to the chargeability parameter m (Fig. 1). Red curve corresponds to the non-polarisable ore body ($m = 0$), light-blue curve is the maximum value of the parameter ($m = 0.9$). Increasing chargeability leads to changing amplitude and a shape of the apparent resistivity curves. The curve corresponding to the value $m = 0.9$ is so deformed by influence of induced polarisation that looks like a two-layer medium without ore body. The parameter c is equal to 0.5.

Then we change the time constant parameter τ (Fig. 2, left diagram). This parameter ranges from 0.1 to 15 seconds. Other parameters have the fixed values: $m = 0.5$, $c = 0.5$. It is clear that the maximum is displaced to
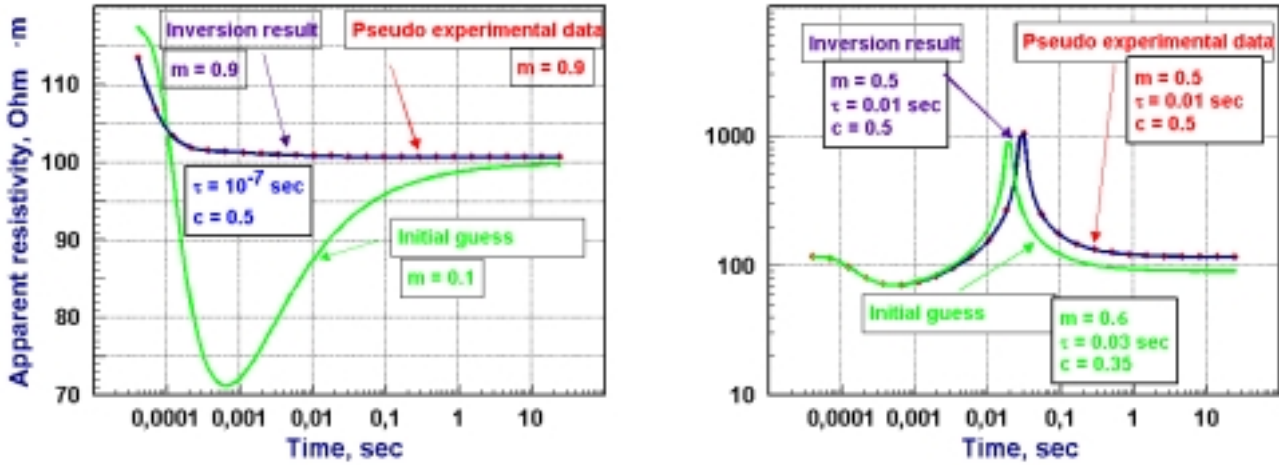
FIG. 3. One-parametrical (on the left) and three-parametrical (on the right) minimisation.
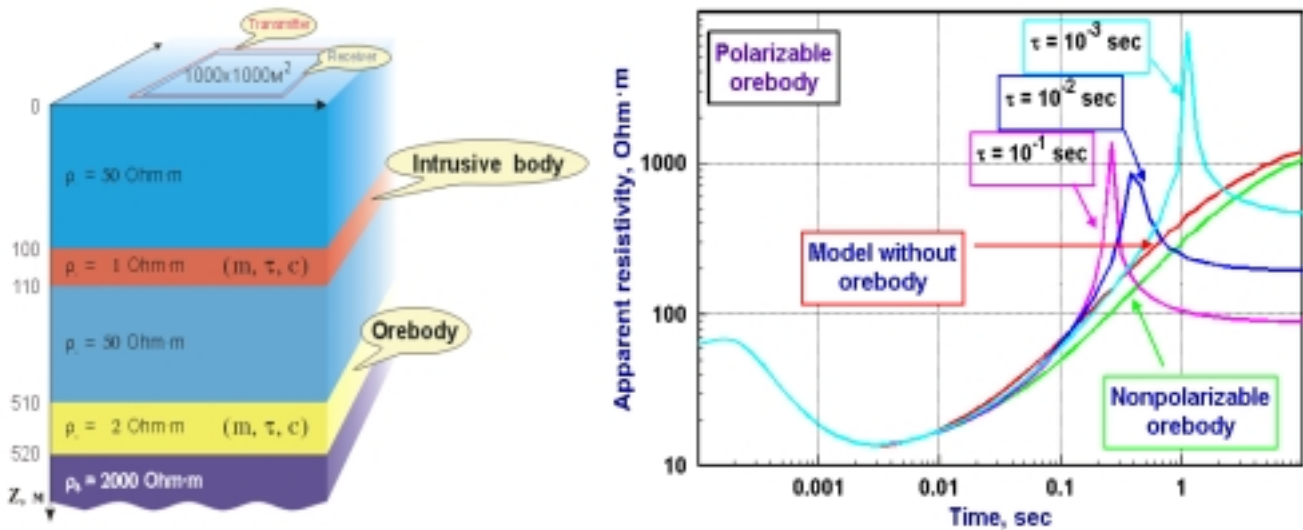

FIG. 4. Geoelectrical model (on the left) and the high-resolution behaviour (on the right).

the long-time region with increasing the time constant. The same numerical experiment (Fig. 2, right diagram) with the frequency-dependence $c = 1.0$ shows two extremes on the apparent resistivity curves. The signal being measured passes twice through a zero.

Significant influence of ore body polarisation on the medium response allows one to hope for reliable work of the inversion algorithm. The modified simplex-method has been used for the solution of inverse problem. The residual function is determined by the least square method. Some coordinate transformation on a positive real half-axis (as the simplex method requires) has been performed for the reduction of polarisation parameters to the same scale and for searching the solution of inverse problem. The noise is considered as irregularly distributed and that is less than 1% in all examples given in the paper.

In Figure 3, an example of reconstruction of the chargeability (m) is shown. The true value (0.9) is shown by a red curve. The initial value of m is equal to 0.1 (green curve). The result of interpretation (blue curve, $m = 0.9$) completely agrees with the true value of chargeability.

A more complicated three-dimensional inverse problem for the same IP ore body model (Fig.3, on the right) has been exercised. Pseudo-experimental data (red curve) correspond to the following values of Cole-Cole parameters: $m = 0.5$, $c = 0.5$, $\tau = 0.01$ sec. The initial model (blue curve) differs slightly from the true value by the value of m = 0.6. However, the initial value of $\tau = 0.03$ differs three times and the initial value of $c = 0.35$ differs by a factor of 1.5 from the true values, respectively. After more than 100 iterations, the
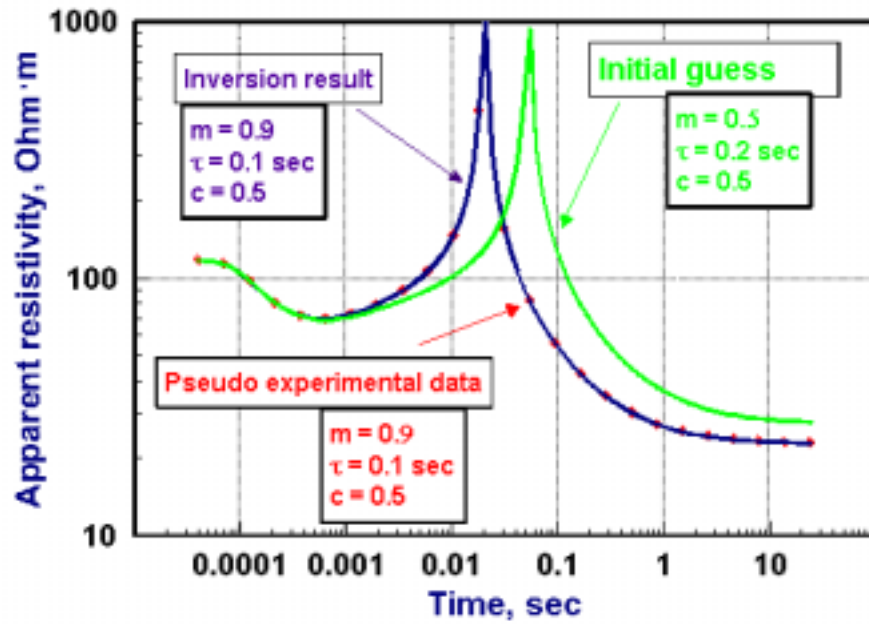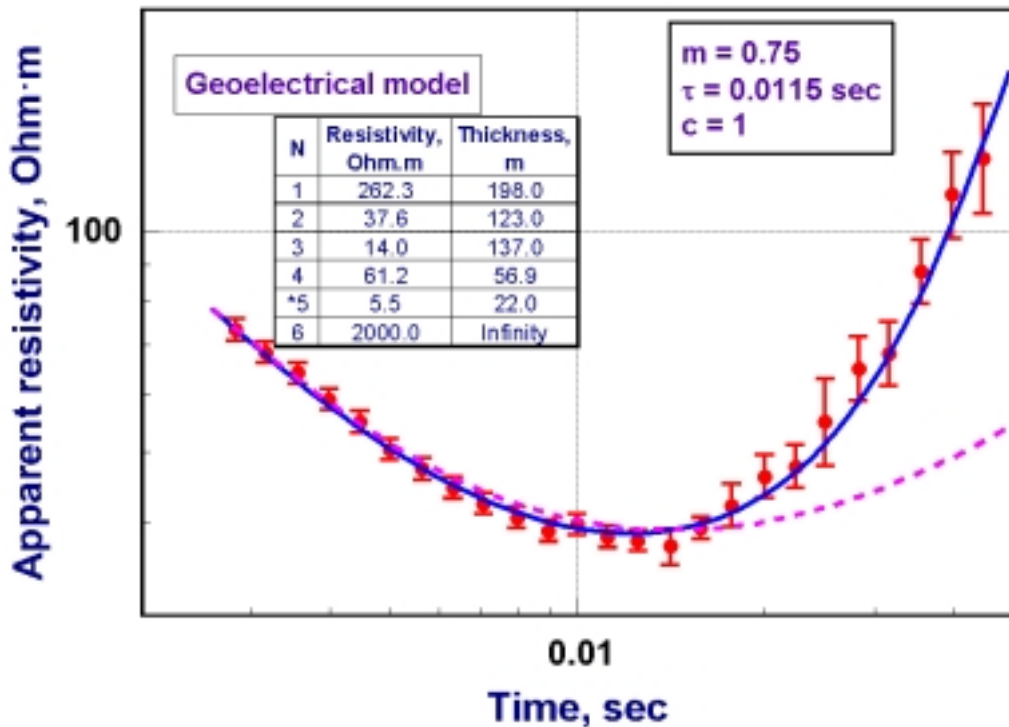
FIG. 5. Two-parametrical minimization.

FIG. 6. Inversion of the experimental data.

final inversion result is $m = 0.5$, $c = 0.5$, $\tau = 0.01$ that show close agreement with the true values.

We consider a more complicated model that a polarisable ore body overlain by the trap intrusion. The model that consists of five layers (Fig. 3, on the left) exemplifies a high-resolution electromagnetic prospecting.

A series of calculations is given in Fig.4, on the right). The non-polarisable ore body is represented by the red curve. If an ore body is absent in the model, the diagram has green colour. Thus, the ore body response is within the measurement errors. The contribution of the body to the signal becomes important if the ore

body is polarisable. The medium response demonstrates sign changes corresponding to maxima on apparent resistivity curves. Thus, by the presence of polarisation, it is possible trough electromagnetic prospecting to determine the objects, which are invisible when using the purely induction approach.

Finally, we consider an example of two-parametrical model (Fig. 5). Pseudo-experimental data are characterised by the parameters: $m = 0.9$, $c = 0.5$, and $\tau = 0.2$ sec. The chargeability and the time constant are reconstructed by the inversion. The result (blue curve) completely coincides with pseudo-experimental data. The polarisation parameters are recovered with a good accuracy.

The developed algorithm was applied to the inversion of electromagnetic sounding data by TEM method in the Chuya depression (Gorny Altai, Russia). The available geological information indicates that friable deposits of Altai depressions are practically non-magnetic. Enhanced magnetic properties are peculiar for metamorphic and effusive rocks such as tuffs, porphyries, and ultrabasic, which are located at the bottom of a cross-section, whereas the induction sounding data obtained by TEM method in this region cannot be interpreted in the class of models without considering the chargeability of rocks.

Figure 6 illustrates the interpretation of induction soundings with the inclusion of the chargeability. The geoelectrical model consists of six layers with differing values of resistivity. The layer lying at the bottom is characterised by the following chargeability parameters: $m = 0.75$, $\tau = 0.0115$ sec, $c = 1.0$. Drilling data support the results that are obtained from the geophysical data.

CONCLUSIONS

The implemented research shows that the influence of frequency dispersion on the response of a geological medium in the induction arrays may become significant. In many cases, increasing resolution in electromagnetic data can be achieved at the expense of additional induced polarisation parameter introduction in the model. The developed algorithm is based on the simplex method and it solves the polarisation parameters by the inverse method. The successful reconstruction of the frequency dispersion parameters has been done on real survey data.

ACKNOWLEDGEMENTS

REFERENCES

Epov, M.I. and Yeltsov I.N., 1991. Electromagnetic field relaxation of dipole source in conductive layered bed plunged into insulator: Geologya i geofizika, **32**, 110-113.

Flis, M.F., Newman, G.A., and Hohmann, G.W., 1989. Induced-polarization effects in time-domain electromagnetic measurements: Geophysics, **54**, 514-523.

Smith, R.S. and West, G.F., 1989. Field examples of negative coincident-loop transient electromagnetic responses modelled with polarizable half-planes: Geophysics, **54**, 1491-1498.

Svetov, B.S., Ageev, V.V. and Lebedeva N.A., 1995. Earth rock polarization and phenomenon of high resolution of geoelectrics: Geofizika, **4**, 42-52 (in Russian).